Toxicology Research

Accepted Manuscript

ROYAL SOCIETY OF CHEMISTRY

www.rsc.org/toxicology

Genotoxic risk of quinocetone and its possible mechanism in *in-vitro* studies

Xu Wang[1], Panpan Yang[2], Juan Li[2], Awais Ihan[4], Qianying Liu[2], Guyue Cheng[2], Yanfei Tao[3], Zhengli Liu[3], Zonghui Yuan[1,2,3]*

[1]National Reference Laboratory of Veterinary Drug Residues (HZAU) and MOA Key Laboratory for Detection of Veterinary Drug Residues, [2]MOA Laboratory for Risk Assessment of Quality and Safety of Livestock and Poultry Products, Huazhong Agricultural University, Wuhan, Hubei 430070, China, [3]Hubei Collaborative Innovation Center for Animal Nutrition and Feed Safety, Wuhan, Hubei, China, [4]Department of Biosciences, COMSATS Institute of Information Technology, Sahiwal, Pakistan.

*Corresponding author: Prof. Dr. Zonghui Yuan, Tel: 86-27-87287186, Fax: 86-27-87672232, E-mail: yuan5802@mail.hzau.edu.cn

Abstract

Quinoxalines (QdNOs) possessing the quinoxaline-1,4-dioxide basic structure were are used for their antibacterial action, although their mechanisms of genotoxicity are not clear. After comparing with the sensitivity of V79 cells and HepG2 cells using quinocetone (QCT) and other QdNOs, it was found that HepG2 cells were more sensitive. The results showed that QCT induced the generation of $O_2^{\bullet-}$ and $OH^{\bullet}$ during the process of metabolism. Free radical could then attacked guanine and induced 8-OHdG generation, causing DNA strand breakage, the inhibition of topoisomerase II (topo II) activity, and impacting *PCNA*, *Gadd45* and *topo II* gene expression. QCT also caused mutations in the mtDNA genes *COX1*, *COX3* and *ATP6*, which might affect the function of the mitochondrial respiratory chain and increase the production of ROS. Nuclear extracts from HepG2 cells treated with QCT had markedly reduced topo II activity, as judged by the inability to convert pBR322 DNA from the catenated to the decatenated form by producing stable DNA-topo II complexes. The study suggested that QCT bound to DNA in a groove and electrostatic combination, and might affect the dissociation of topo II from DNA and impact DNA replication. Taken together, these data reveal that DNA damage induced by QCT resulted from $O_2^{\bullet-}$ and $OH^{\bullet}$ generated in the metabolism process. The data will throw new light onto the genotoxicity of quinoxalines.

***Key words*:** Quinoxalines; DNA adducts; ROS; Mitochondrial DNA mutation; Genotoxicity; Quinocetone

Abbreviations: 8-OhdG, 8-hydroxy-deoxyguanine; AFB1, aflatoxin B1; BCA, bicinchoninic acid; CASP, comet image analysis system; CAT, catalase; CBX, carbadox; CID, collision-induced dissociation; ct-DNA, calf thymus DNA; CY1, N1-deoxy cyadox; CY2, N4-deoxy cyadox; CY5, bi-deoxy cyadox; CY9, quinoxaline-2-carboxylic acid; CYA, cyadox; DAPI, 4'6-diamidino-2-phenylindole; DCFH-DA, 2',7'-dichlorodihydrofluorescein diacetate; DHE, dihydroethidium; DMEM, Dulbecco's Modified Eagle's Medium; DMSO, dimethyl sufoxide; DSBs, double stand break; FBS, fetal bovine serum; FITC, fluorescein isothiocyanate; GPx, glutathione peroxidase; H_2O_2, peroxide; HPLC, high performance liquid chromatographic; LC/MS-ITTOF, ion trap/time-of- flight mass spectrometry; LMP, low melting point; M1, 2-isoethanol mequindox; M2, 2-isoethanol 1-desoxymequindox; M4, bi-desoxy mequindox; M10, 2-isoethanol bi-desoxymequindox; MEQ, mequindox; MQCA, 3-methyl-quinoxaline-2-carboxylic acid; mtDNA, mitochondrial DNA; MTT, methylathiazol tetrazolium bromide; $O_2^{\bullet-}$, superoxide anion radical; OD, optical density; $OH^{\bullet}$, hydroxyl radical; OLA, olaquindox; OTM, olive tail moment; PAH, polycyclic aromatic hydrocarbons; PMSF, phenylmethanesulfonyl fluoride; Q3, N4-deoxy quinocetone; Q4, N1-deoxy quinocetone; Q5, N4-deoxy quinocetone; Q6, bi-deoxy quinocetone; Q7, 3-methyl-2- quinoxalinebenzenevinylalcohol; QCT, quinocetone; QdNOs, ROS, reactive oxygen species; SCGE, single cell gel electrophoresis; SLS, sodium N-lauroylsarcosine; SOD, superoxide dismutase; SSBs,

68 single strand break; TARDIS, trapped in agarose DNA immunostaining; topo II,
69 topoisomerase II; TPZ, tirapazamine; VP-16, etoposide; X/XOR, xanthine/xanthine
70 oxidase
71

1 Introduction

Quinoxaline-1,4-dioxides (QdNOs) are widely used as antibacterial drugs [1] and possess broad bioactivity.[2] Carbadox (CBX) and olaquindox (OLA) have been banned by European Commission because of their potential properties of inducing cancer via genetic aberrations and mutation.[3] Mequindox (MEQ) and quinocetone (QCT) are new members of the QdNO family and there have been only a few reports about their potential genotoxicity.[4-6]

In previous studies, the genotoxicity of QdNOs was found to be closely related to the production of reactive oxygen species (ROS). MEQ genotoxicity is attributable, in part, to its role as a potent inducer of DNA damage via ROS.[7] QCT has toxic effects on HepG2 cells and results in the induction of mitochondria-dependent and mitochondria-independent pathways of apoptosis.[8, 9] The previous research has shown that ROS play an important role in DNA damage induced by QCT [10, 11] and OLA.[12, 13] QCT increase the generation of ROS in the liver and kidney, and decrease superoxide dismutase (SOD) and catalase (CAT) activity.[14] However, the source of ROS and the relationship between DNA damage and ROS induced by QdNOs are still far from clear. Furthermore, there are some other factors that could cause DNA damage induced by quinoxalines, such as topoisomerase inhibition and DNA adducts, which should also be considered.[15]

ROS are mainly composed superoxide anion radicals ($O_2^{\bullet-}$), hydroxyl radicals ($OH^{\bullet}$), and hydrogen peroxide (H_2O_2). These compounds attack DNA, carbohydrates and proteins, and cause DNA double strand breaks, affect enzyme activity and lead to

many kinds of toxic reactions.[16, 17] ROS mainly originate in the mitochondria and maintain normal life activities.[18-21] If mitochondrial DNA is damaged, ROS are generated excessively.[22] Equally, certain exogenous chemicals might induce the redox cycle following metabolism in cells, with the subsequent production of electrons that could be transferred to molecular oxygen, producing superoxide.[23] $O_2^{\bullet-}$ can be converted to $OH^{\bullet}$ by SOD, and is the most toxic free radical.[24] Previous research has implied that the toxicity of quinoxalines is related to *N*-oxide group reduction and the generation of ROS.[2] Whether this supposition is correct requires further analysis. Moreover, the source of the ROS generated by QdNOs and the exact species of ROS also remain unclear.

Topoisomerase II (topo II) plays an important role in DNA replication and repair. It changes DNA topology during the DNA replication process and keeps the replication fork moving forward.[25] Topomerase α and β are responsible for unwinding DNA in two ways, i.e. double stand break (DSBs) and single strand break (SSBs).[25] There are many topoisomerase inhibitor drugs which inhibit topoisomerase activity and cause irreversible DNA damage, including adriamycin and etoposide. These compounds block the religation stage, and thereby generate frank DSBs.[26] Drugs that stabilized topo II with DNA DSBs are termed topo II poisons.[26] Tirapazamine (TPZ), one of the QdNOs, has anticancer activity because it is a tumor-specific topo II poison.[27]

There are some interactions between DNA and drugs, such as non-covalent binding (groove, embedded or electrostatic) and covalent binding.[28] No matter what

the interaction between DNA and drugs, these cause DNA damage that cannot be easily repaired. [29] Genes, such as *POLB, PCNA, topo II, Gadd45, DNA-PK, RPA3, OGG1, RFC, CDC6, RAD50* and *BRCA1* play roles in DNA replication and repair. [30-33] When physical or chemical factors affect their expression, this leads to DNA damage [12] and impacts DNA replication. [34]

QdNOs have variable mutagenic toxicity. 3-methyl-quinoxaline-2-carboxylic acid (MQCA), as the residue of OLA also causes DNA strand breaks. [35] The genotoxic sensitivity of mammalian cells to quinoxalines is not consistent. [36] Therefore, investigations into genotoxic metabolites and screening the most sensitive cells and most toxic quinoxaline compounds are necessary (Fig. 1). Quinoxalines have similar genotoxicity via causing DNA strand breaks [7]; therefore DNA strand break was chosen as an indicator of toxicity. HepG2 cells and V79 cells are commonly used in toxicology research studies than human normal liver cells (L02 cells) or animal primary cells. Furthermore, because the mutagenicity of QdNOs under lower oxygen condition was stronger than those under aerobic condition, HepG2 cells seemed to be more suitable than L02 cells. [13, 37, 38] MTT and single cell gel electrophoresis (SCGE) were used to determine the most genotoxic quinoxaline compound and the most sensitive cell (HepG2 or V79 cells).

QCT was found to be the most genotoxic compound. It was hypothesized that QCT would be metabolized and generate $O_2^{\bullet-}$ and $OH^{\bullet}$, which play an important roles in DNA damage. A dihydroethidium, 7'8'-dihydro-8-oxodeoxyguanosine (8-OH-dG) ELISA kit and the SCGE method were used to detect $O_2^{\bullet-}$ and $OH^{\bullet}$, respectively.

Because the structure of QCT is similar to that of TPZ, it was thought that QCT might be a topo II poison, as is TPZ. Therefore, the nuclei from mammalian cells treated with QCT were extracted to detect topoisomerase activity. Considering the fact that OLA and CBX can interact with plasmids and induce mutations [39], it was hypothesized that QCT would interact with DNA and cause DNA strand breaks and mutations. Moreover, the gene expression of DNA replication and repair enzymes was assessed to investigate the relationship between DNA damage and the inhibition of gene expression. These results shed new light on the mechanism of genotoxicity of QdNOs, which will help to use currently available drugs and to push the development of novel compounds with more efficient potential and fewer harmful effects.

<Insert Fig. 1 here>

2 Materials and methods

2.1 Chemicals and reagents

Olaquindox (OLA, 99%), mequindox (MEQ, 99.8%) and quinocetone (QCT, 99%) were purchased from Zhongmu Pharmaceutical Co. Ltd. (Wuxue, PR China). Carbadox (CBX, 98%) was purchased from Sigma Chemical Co. (St. Louis, MO, USA). Cyadox (CYA, 99.8%) was obtained from the Institute of Veterinary Pharmaceuticals, Huazhong Agricultural University (Wuhan, PR China). All the metabolites (purity, 99%) were obtained from the Department of Veterinary Pharmacology and Toxicology, China Agricultural University (Beijing, PR China). All five compounds and their metabolites were dissolved in dimethyl sulfoxide (DMSO,

Amresco, USA) and then diluted in Dulbecco's modified Eagle's medium (DMEM, Hyclone, Logan, USA) at the desired concentrations. Collagenase (type IV, 268 U/mg) and 3-(4, 5-dimethylthiazol-2-yl) -2, 5-diphenyltetrazolium bromide (MTT) were obtained from Gibco-BRH (Gibco, Grand Island, NY, USA). Methylthiazoletrazolium, phenylmethanesulfonyl fluoride (PMSF), dihydroethidium, 2′,7′-dichlorodihydrofluorescein, dimethyl sulfoxide, dAMP, dTMP, dCMP and dGMP were purchased from Sigma (St. Louis, USA). A human 8-OHdG ELISA kit was obtained from CUSABIO (Wuhan, PR China). Human topo II and human topo II α polyclonal antibodies were provided by Topogen Inc. (Columbus, OH, USA). pBR322 DNA was obtained from Beijing Huaxia Ocean Science and Technology Co., Ltd. (Beijing, PR China). All other chemicals and reagents were of high analytical grade.

2.2 Cell culture

HepG2 cells and V79 cells were purchased from the Shanghai Institutes for Biological Sciences, Chinese Academy Cell Resource Center (Shanghai, PR China). HepG2 cells and V79 cells were cultured in DMEM and RM1640 supplemented with 10% fetal bovine serum (FBS), respectively. Cultures were incubated at 37 °C in a humidified atmosphere with 5% CO_2.

2.3 Cell viability

HepG2 cells and V79 cells (5×10^4/mL) were seeded in 96-well flat-bottomed plates and allowed to adhere for 12 h. Cells were treated with quinoxalines and their metabolites at 5, 10, 20, 40, 80 and 160 μM for 0.5, 1, 2, 4 and 8 h, respectively.

These compounds got easily dissolved in DMSO, and they were diluted with cell culture medium to the concentration indicated with a final DMSO concentrations of ≤ 0.1% (v/v). The cells were treated with 0.1% DMSO as a control. Thereafter, the cells were treated with a final concentration of 0.5 mg/mL MTT and incubated at 37 °C for 4 h. The purple formazan crystals were dissolved in 150 μL of DMSO. Then, the optical density (OD) was measured using a Microquant plate reader (Bio-Tek Instruments) at 570 nm. Cell viability in response to treatment with drugs was calculated as: Cell Viability = (OD of sample well - OD of control well) /(OD of control well - OD of blank well).

2.4 DNA strand break analysis using the SCGE assay

DNA strand break was detected using a protocol for the alkaline comet assay described by Singh and Bhat (2012).[40] Ten microliters of the cell suspension (approximately 10^6 cells) was mixed with 130 μL of 0.8% low melting point (LMP) agarose melted in PBS in Eppendorf tubes at 38 °C. The slides, with coverslips removed, were then immersed in a cold, freshly prepared lysis solution [2.5 mol/L NaCl, 100 m mol/L EDTA, 10 m mol/L Tris, 1% sodium N-lauroylsarcosine (SLS) with pH 10, 1% Triton-100 and 10% DMSO added freshly prior to use] for 4 h in the refrigerator. After lysis was completed, the slides were rinsed with distilled water and then were placed in a horizontal gel electrophoresis box containing fresh, chilled electrophoresis buffer to a level 0.25 cm above the slides. The slides were left for 20 min to let the DNA fully unwind so that alkali-liable damage could be expressed.

Electrophoresis was conducted at 4 °C for 20 min at 25 V and 300 mA. Slides were drained and neutralized with three changes of neutralization buffer (0.4 M Tris, pH 7.5), each time for 5 min to remove the detergent and alkali. The slides were removed from the neutralization solution, rinsed gently, and then stained with 40 μL of 20 μg/mL ethidium bromide. Slides were observed at a magnification of ×400 using a fluorescent microscope (Olympus, CK40) equipped with a BP546/10 excitation filter and a 590 nm barrier filter. On each replicate slide, 100 cells were scored (200 cells total for each concentration) using a comet image analysis system (CASP). Data on tail length, tail moment and the DNA content of comet tail were recorded. Only cells with a defined head were scored, and dead cells were excluded.

2.5 The integration analysis of DNA with QCT

The integration analysis of DNA with QCT was performed as described previously.[41, 42] Calf thymus DNA (ct-DNA) (12.5, 25, 50, 100 and 200 μM) was treated with 40 μM of QCT for 4 h, respectively. The integration was detected by UV-visible absorption spectra (Beijing Purkinje General Instrument Co., Ltd, PR China). The value of absorption peak was observed by UV scanning from 200 nm to 400 nm.

After 4 h incubation with 12.5 mg/mL of dAPM, dTMP, dCMP and dGMP with 40 μM of QCT, respectively, the reaction products were detected using HPLC (Shimadzu Corporation, Kyoto, Japan). A Waters Symmetry C-18 column (5 μm, 4.6×250 mm) was used for detection of the samples. The mobile phase consisted of A

(methanol) and B (0.1% formic acid– 0.032% ammonium formate aqueous solution) with gradient elution. From 0 to 40 minutes, the mobile phase was A (6~50%) and B (94~50%), and from 40-50 minutes, the mobile phase was A (50~6%) and B (50~94%). The flow rate was 0.7 mL/ min. The column was maintained at 46 °C, and the injection volume was 30 μL. No endogenous or extraneous peaks were observed interfering with the separation.

2.6 Generation of ROS analysis using the fluorescence probe assay

ROS generation was measured with 2',7'-dichlorodihydrofluorescein diacetate (DCFH-DA) assay described by Eruslanov and Kusmartsev (2010).[43] Following exposure to the drug (5, 10, 20, 30 and 40 μM) for 0.5, 1, 2, 3 and 4 h, the cells were trypsinized and washed with ice-cold PBS. Then, 1 mL of PBS containing 20 μM DCFH-DA were added, and the cells were incubated for 30 min at 37 °C. The fluorescence emission from DCF was analyzed using a fluorescence microplate reader (BioTek Instruments, Winooski, VT, USA) with excitation and emission spectra set at 480 and 530 nm, respectively.

2.7 Generation of $O_2^{\bullet-}$ using a fluorogenic probe assay

$O_2^{\bullet-}$ was measured using the dihydroethidium (DHE) assay as described by Peshavariya with some modifications.[44] $O_2^{\bullet-}$ generation resulted from the incubation of QCT with xanthine oxidoreductase (XOR). After exposure to the drug (10, 20, 40, 80 and 160 μM) for 4 h, and then treatment with XOR (50 μM) at 37 °C for 30 min,

244 the OD values were determined at 580 nm.

245 After the cells were exposed to 0, 5, 10, 20, 30 and 40 μM of QCT or Q6 or SOD
246 (3.25 U/μL) for 4 h, the culture medium was removed and PBS was added. DHE (1
247 μM) was added to the cells culture well and incubated for 30 min. Then, cells were
248 collected and centrifuged at 1500×g for 5 min three times. Cells were resuspended in
249 PBS and added to 96-well plates. Changes in fluorescence were monitored with a
250 multiwell plate reader for 10 min at 37 °C. Data are expressed as the net increase in
251 fluorescence.

252 ***2.8 LC/MS-ITTOF analysis of the metabolites of QCT***

253 HepG2 cells were incubated with 20 μM of QCT at 37 °C for 4 h. QCT and its
254 metabolites in the cell or supernatant samples were detected by using hybrid IT/TOF
255 mass spectrometry coupled to a high-performance liquid chromatography system
256 (LC/MS-ITTOF) (Shimadzu Corp., Kyoto, Japan). The liquid chromatography system
257 (Shimadzu) was equipped with a solvent delivery pump (LC-20AD), an autosampler
258 (SIL-20AC), a DGU-20A_3 degasser, a photodiode array detector (SPD-M20A), a
259 communication base module (CBM-20A) and a column oven (CTO-20AC).

260 The cells were collected and centrifuged at 1500×g for 10 minutes. After adding
261 200 μL of PBS, cells were lysed using a CV18 ultrasonic cell disruption device from
262 Nanjing Xinchen Biological Technology Co., Ltd. (Nanjing, PR China).
263 The lysed product was centrifuged at 10,000×g for 15 minutes after adding 200 μL of
264 methanol. Then, the supernatant was collected, and 10 mL of acetonitrile was added

and vortex mixed for 5 minutes. After vigorous shaking, followed by centrifugation at 10,000×g for 15 minutes, the supernatant was dried under N_2 in a 35 °C water bath. The residue was reconstituted in 5 mL of distilled water. The total supernatant was applied to a methanol and water pre-washed HLB 3cc cartridge (Waters Corporation, Milford, Mass U.S.A). The samples were then sequentially washed with 3.0 mL of water and 5% methanol in water. The cell extracts were eluted into plastic tubes with 5 mL of methanol. The eluate was evaporated to dryness under nitrogen at 35 °C and the samples were reconstituted in 500 µL of a methanol: water (40:60 v/v) solution and passed through a 0.22 µm filter membrane for LC/MS –ITTOF. HPLC separation was performed as described above except an isocratic solvent mixture composed of 75% water, 25% acetonitrile, and 0.1% phosphoric acid was used at a flow rate of 0.2 mL/min. Positive ion electrospray was used as the means of ionization and collision-induced dissociation (CID) using argon gas. Other instrument settings included a capillary voltage of 4.5 kV, a capillary temperature of 200 °C and a column temperature of 40 °C. The separation was performed on a Zorbax eclipse XDB-C18 column (150 mm×2.1 mm, 3.5 µm) using gradient elution consisting of mobile phase A (0.1% formic acid in water) and mobile phase B (acetonitrile). The gradients were 5% B-20% B (0-16 min), 35% B (25 min), 60% B (30 min), 100% B (35-37 min), 5% B (37.1 min), 5% B (45 min). The injection volume was 10 µL. The flow rate was 0.2 mL/min, and the wavelength used was 306 nm.

2.9 Effect of QCT metabolism on DNA damage

A xanthine/xanthine oxidase (X/XOR) enzyme system as an one-electron reducing agent for the activation of QCT was used to investigate the effect of the metabolism of QCT on DNA damage under aerobic and low oxygen conditions (Table S1, S2). In this assay, DNA strand scission was readily measured by observing the conversion of supercoiled (form I) plasmid DNA to the open circular form (form II) resulting from nicking the DNA backbone. Assays were prepared in an inert atmosphere glove bag and the solutions were freeze-pump-thaw degassed or purged with inert gas to remove molecular oxygen. The final concentrations of DNA, xanthine, XOR, QCT, TPZ and SOD were 0.05 μg/μL, 100 μM, 8.75 U/mL, 160 μM, 500 μM and 3.25 U/μL, respectively. After incubation at 37 °C for 2 h, and the whole content was observed in a 1% agarose gel stained with ethiduim bromide after electrophoresis for 1 h.

2.10 Topo II activity analysis

Nuclear extracts were prepared as described with some modifications.[27] Briefly, untreated HepG2 cells were pelleted and lysed in 1.0 mL of nuclear buffer A [1 mmol/L KH_2SO4, 150 mmol/L NaCl, 5 mmol/L $MgCl_2$, 1 mmol/L EDTA, 0.1 mmol/L PMSF, 0.1 mmol/L DTT, and 10% glycerol (v/v)]. After initial lysis, the cells were rinsed with nuclear buffer A and spun at 460×g for 10 min. Pelleted cells were resuspended in 1.0 mL of nuclear buffer A and 9.0 mL of nuclear buffer B (nuclear buffer A containing 0.3% Triton X-100). Samples were gently rotated for 10 min and spun at 460×g for 10 min. After centrifugation, the supernatants were removed and

centrifuged again at 12000×g for 15 min. The supernatant was obtained and the protein content was determined using a bicinchoninic acid (BCA) protein assay kit (Beyotime, Shanghai, PR China).

Topo II activity was assayed as described.[27] Reactions contained 0.1 μg pBR322DNA, 50 mmol/L Tris-HCl, 120 mmol/L KCl, 10 mmol/L $MgCl_2$, 0.5 mmol/L of DTT, ATP, and 1 μL 2U/μL topo I and topo II. The reactions were incubated for 30 min at 37 °C and terminated with 1 μL proteinase K and 2 μL 10% SDS. Samples were extracted once with an equal volume of chloroform: isoamyl alcohol (24:1). Following brief centrifugation in a microfuge, the blue upper layer was loaded directly onto an agarose gel. The decatenation products were analyzed on 1% agarose gels run either without or with 0.5 μg ethidium bromide as specified. Electrophoretic analyses of kDNA were performed using standard gel electrophoresis units.

The trapped in agarose DNA immunostaining (TARDIS) assay was performed as described by Willmore et al. with some modifications.[45] Slides were stained with anti-topo II rabbit polyclonal antibody (1:100; TopoGEN, TG2010-1) in PBS containing 0.1% Tween 20 and 1% BSA for 1 h at room temperature. Slides were then stained with FITC-conjugated goat antirabbit IgG antibody in PBS containing 0.1% Tween 20 and 1% BSA for 1 h at room temperature and treated with DAPI and Hoest33258 for 5 min and visualized using a fluorescent microscope (Olympus, CK40).

2.11 Mutation of mtDNA analysis using sequence analysis

mtDNA was isolated as described earlier.[46] The samples were digested with proteinase K and ethanol precipitated. The quality of the DNA was checked by PCR for β globin as an internal control. The DNA was used to amplify the entire region of the mitochondrial genome. The mtDNA was amplified using the forward and reverse primers shown in Table 1.

<Insert Table 1 here>

Briefly, 50 ng of extracted DNA was amplified in a 25 μL final reaction volume under the following conditions: 1×DNA polymerase buffer [16 mmol/L of $(NH_4)_2SO_4$, 67 mmol/L of tris-HCl (pH 8.8), 0.1% polysorbate], 1.5 mmol/L of $MgCl_2$, 500 nmol/L of each primer, and 1 U of Super Taq. PCR conditions were as follows: 94 ℃ for 5 min; 30 cycles at 94 ℃ for 30 s, 58 ℃ for 30 s, and 72℃ for 40 s; and a final extension step at 72 ℃ for 5 min. Next, the total PCR products were purified and sent to Wuhan Anygene Biotechnology Corporation Limited (Wuhan, PR China) to analyze the sequence.

2.12 Expression of mRNA assay using RT-PCR

Total cellular RNA was isolated from the cells with a few minor modifications.[47] The purity of RNA sample was defined by the A260/A280 ratio. One microgram of RNA was reverse transcribed to cDNA with the ReverTra Ace™ First Strand cDNA Synthesis Kit (Promega, Madison, WI, USA). cDNA was amplified by qRT-PCR (BioRad, Hercules, CA) using SYBR Premix Ex Taq RT-PCR kit (Takara, Code

BKA701, China). Each 25 μL reaction mixture consisted of 12.5 μL SYBR Premix Ex Taq, 0.5 μL of each primer (10 μM), 2 μL of cDNA, and 9.5 μL RNase-free dH_2O. Cycling conditions were as follows: step 1, 30 s at 95 ℃; step 2, 45 cycles at 95 ℃ for 5 s, 60 ℃ for 30 s; step 3, dissociation stage. The endpoint used was real-time PCR quantification. Relative quantification of gene expression was calculated using the $2^{-\Delta\Delta Ct}$ data analysis method, as previously described [48] and normalized to GAPDH in each sample. Primers used in this study are provided in Table 2.

<Insert Table 2 here>

3 Results

3.1 The effects of drugs on cell viability

Dose and time-dependent increases in cytotoxicity occurred when HepG2 cells and V79 cells were exposed to the drugs (data not show). It was found that cell viabilities induced by 40 μM QCT, CBX, OLA and MEQ for 4 h were 76.40±4.50%, 83.50±2.60%, 80.20±5.40% and 84.50±6.60%, respectively, indicating that QCT presented greater cytotoxicity than the other parent drugs. Furthermore, the MTT results also show that the parent drugs had more toxicity than their metabolites. Similar results were observed in V79 cells after treatment with QdNOs and their metabolites. Doses of 10-160 μM for QdNOs and their metabolites were selected for future studies based the MTT results.

3.2 Appraisal of the most sensitive cells and the genotoxicity of quinoxaline compounds by the SCGE assay

Total DNA strand breaks in HepG2 cells and V79 cells were analyzed by the comet assay. Experiments were performed on QdNOs and their metabolites at 40 μM for 4 h. The data demonstrate that CBX, OLA, MEQ, QCT and their metabolites all induced DNA strand breaks. The results are summarized in Fig. 2. Tail-DNA% and Olive Tail Moment (OTM) were used as the indices of DNA strand breaks. The OTM of HepG2 cells and V79 cells was 14.66±3.12% and 9.82±2.88% for CBX, 25.00±3.44% and 12.40±4.82% for QCT, 22.50±2.68% and 18.85±3.08% for OLA, respectively with 40 μM exposure for 4 h. The results suggest that HepG2 cells were more sensitive to the quinoxaline compounds than V79 cells. The ability of the parent drugs to induce DNA strand breaks was greater than their metabolites. QCT showed the most potential ability to induce DNA strand breaks. Therefore, QCT was chosen as the most genotoxic compound among the QdNOs and their metabolites.

DNA strand break induction by QCT was assessed in a dose and time-effect relationship. Three time points and five concentrations of QCT were selected to investigate the ability to induce DNA strand breaks.

<Insert Fig. 2 here>

3.3 The interaction of DNA with QCT

The absorbance values of DNA and QCT were 260 and 317 nm, respectively.

Following the increased concentration of ct-DNA, the absorbance value of QCT increased and a hyperchromic effect occurred. The maximum UV absorption wavelength of ct-DNA was offset by 3 nm in the shortwave direction, indicating that QCT interacted with ct-DNA in a non-intercalative mode. The interaction of dAMP, dTMP, dCMP and dGMP with QCT was detected. The results show that QCT could not combine with them, and therefore no covalent interaction occurred between QCT and DNA (Fig. 3).

<Insert Fig. 3 here>

3.4 Generation of ROS, $O_2^{\bullet-}$ and metabolites induced by QCT

The results show that QCT induced intracellular ROS generation in a time- and dose-dependent fashion (Fig. 4A). The amount of $O_2^{\bullet-}$ generation by HepG2 cells occurred in a dose-dependent manner (Fig. 4B). The results show that QCT could induce intracellular $O_2^{\bullet-}$ generation in a dose-dependent fashion with the catalysis of XOR, suggesting that XOR plays an important role in the production of $O_2^{\bullet-}$ (Fig. 4C). Fig. 4D shows that QCT induced HepG2 cells to generate $O_2^{\bullet-}$, and SOD significantly eliminated the free radical.

Additionally, the results confirm that $OH^{\bullet}$, one of the most highly reactive ROS, was generated by HepG2 cells treated with QCT. Some studies have suggested that $OH^{\bullet}$ can attack DNA and generate 8-OHdG. In the present study, 8-OHdG levels increased in a dose-dependent manner after treatment with QCT at various concentrations for 4 h (Fig. 4E). Compared with the control, Q6 did not induce the

412 generation of $O_2^{\bullet-}$, while QCT treatment resulted in a significant increase in $O_2^{\bullet-}$
413 production, suggesting that N-O groups play critical role in the generation of $O_2^{\bullet-}$ (Fig.
414 4F). It was also found that N4-deoxy quinocetone (Q3), N1-deoxy quinocetone (Q4)
415 and Q6 was generated by HepG2 cells, indicating that the reduction of the N-O group
416 might be the reason for the generation of ROS and $O_2^{\bullet-}$ (Fig. 4G,H).

417 <Insert Fig. 4 here>

418 ***3.5 The effect of the metabolism process of QCT on DNA damage***

419 It was found that QCT, in conjunction with the X/XOR system, caused direct
420 single-strand breaks in DNA (Fig. 5). In the absence of QCT or X/XOR, there was no
421 significant effect on plasmid DNA, indicating that X/XOR plays an important role in
422 the DNA damage induced by QCT. The DNA damage induced by QCT was similar to
423 the positive control TPZ, suggesting that the metabolism of QCT with X/XOR
424 resulted in DNA damage. Without the presence of QCT, both DMSO and SOD
425 showed no significant effect on DNA integrity. DMSO, a scavenger of $OH^{\bullet}$, led to a
426 significant decrease in DNA damage induced by QCT, indicating that $OH^{\bullet}$ was the
427 free radical attacking DNA. While SOD, a scavenger of $O_2^{\bullet-}$, contributed to DNA
428 damage induced by QCT. It was presumed that, during the process, SOD contributed
429 to converting $O_2^{\bullet-}$ to $OH^{\bullet}$, which has a highly toxic effect on DNA. Additionally, it
430 was found that plasmid DNA breakage was more obvious under low oxygen
431 conditions than that under aerobic conditions.

432 <Insert Fig. 5 here>

3.6 The relationship between topo II activity inhibition and DNA strand breaks induced by QCT

Topoisomerase activity analysis was performed *in vitro*. Topo I and II and pBR322 DNA were treated with various concentrations of QCT to determine whether topo II could support the decatenation of pBR322 DNA. It was found that QCT markedly reduced topo II activity as judged by the inability to convert pBR322 DNA from the catenated form to the decatenated form, whereas the activity of topo I was not changed.

In the TARDIS assay, topo II, covalently attached to DNA, was detected by staining cells with anti-topo II antibodies and secondary antibodies conjugated to FITC. In untreated HepG2 cells, little staining for anti-topo II was present, but significant staining for topo II was observed when the cells were treated with QCT (Fig. 6).

<Insert Fig. 6 here>

3.7 Mutation of mitochondrial DNA

Mitochondrial DNA was extracted using the high-concentration-salt precipitation method. HepG2 cells were treated with QCT at a concentration of 40 μM, for 4 h. Then, HepG2 cells were cleaved and the mitochondrial DNA was extracted. Sequence analysis showed mutations to the *ATP6*, *COX1* and *COX3* genes (Table 3).

<Insert Table 3 here>

3.8 Influence of gene expression of DNA replication and repair

HepG2 cells were treated with QCT at different concentrations for 4 h. The results show that QCT decreased the levels of expression of many genes, but these were not significantly changed after exposure at 10 μM and 20 μM. When cells were exposed to 20 μM QCT for 4 h, the expression of *PCNA* and *topo II* decreased significantly by over two-fold and a two-fold increase in *Gadd45* expression was found compared with the control group, this does was then chosen to investigate the time-effect relationship. The results show that the expression of *PCNA*, *topo II* and *Gadd45* exhibited a time-effect relationship. In addition, SOD significantly weakened the influence of QCT on gene expression.

<Insert Fig. 7 here>

4 Discussion

A number of studies have clearly shown that QdNOs are potentially genotoxic agents, but little is known about their genotoxic mechanism. In the present study, it was found that QCT was the most genotoxic agent among the quinoxalines by SCGE analysis. It was first identified that $O_2^{\bullet-}$ and $OH^{\bullet}$ were generated during the process of *N*-oxide group reduction of QCT by XOR in the cytoplasm. Furthermore, in the present study, it was found that quinoxalines could also interact with DNA, inhibited the dissociation of DNA-topo II complex, significantly changed gene expression related to DNA repair and caused DNA strand breaks (Fig. 8).

The mutagenic and antibacterial activity of prototype QdNOs and the metabolites was enhanced under anaerobic conditions. [37, 38] In the present study, these QdNOs derivatives were compared the genotoxicity in normal cells (V79) and cancer cells (HepG2), and it was found that HepG2 cells were more sensitive to QdNOs. HepG2 is a kind of cancer with low oxygen condition, which might be one of the important reasons that HepG2 cells were more sensitive to the hypoxia-activated compounds, such as QdNOs. In addition, some QdNOs (eg, TPZ, DCQ) were used as anticancer and hypoxia-selective drugs on human. [49, 50] The results might state that QCT presented the hypoxia-selective DNA cleavage, and indicated that QCT might have the potential anticancer activity.

Some studies suggested that the potential of genotoxicity of QdNOs was closely related to the *N*-oxide group reduction. [9, 51] The *N*-oxide reduction progress of QdNOs might lead to the formation of ROS and oxidative stress. [7, 52] In the present study, the genotoxicity potential of prototype drugs was significantly higher than that of the metabolites, identifying the important role of the *N*-oxide group in the genotoxicity of QdNOs. However, in the present study, it was found that some *N*-oxide group reduction metabolites (eg. Q6) could induce DNA strand break, suggesting that the genotoxic mechanism of Q6 might be different from that of QCT. It was previously reported that Q6 (5-20 μg/mL) could induce cell cycle arrest at the S phase in Chang liver cells, while the same doses of QCT could not, indicating S phase arrest induced by Q6 might be one reason for its genotoxicity. [53] However, the reason why Q6 induced S phase arrest remains unknown. Although the metabolites

were less toxic than their parent drugs, residual amounts of these chemicals in animal products might pose a hazard to consumer health, and their function on the toxic mechanism and mutagenicity tests should be further carried out.

Oxidative DNA damage induced by ROS is the most important type of damage to DNA.[54] Usually, the generation of 8-OHdG and ROS are considered to indicate oxidative DNA damage.[55, 56] In a previous study, OLA was reported to induce oxidative DNA damage.[12] However, the genetic mechanism of QCT is far from clear. In the present study, it was observed that the generation of ROS occurred in a dose and time-dependent relationship. In the ROS generation and SCGE assay, ROS was found to play an important role in DNA strand breaks in HepG2 cells induced by QCT. As the primary species of ROS, $O_2^{\bullet-}$ was detected for the first time when cells were treated with QCT. ROS are produced excessively in animals and humans when XOR and catecholamine increase, or by chemical substances generated during metabolism.[57] A number of reports have suggested that the toxicity of quinoxalines is related to *N*-oxide group reduction.[2, 58] XOR, cytochrome p450 and aldehyde oxidase have been suggested to be the major metabolic enzymes of quinoxalines;[59] they are located in the cytoplasm, endoplasmic reticulum and mitochondria, respectively. XOR has been found to be responsible for *N*-oxide group reduction.[60] In the present study, MS analysis showed that the desoxy-quinocetone was detected in HepG2 cells treated with QCT, indicating that QCT can enter cells and induce *N*-oxide group reduction. At the same time, there was excessive $O_2^{\bullet-}$ and 8-OHdG generation in the cytoplasm induced by QCT. Here, ROS generation induced by quinoxalines was identified for

519 the first time. Furthermore, guanine in the cytoplasm was easily attacked by $OH^{\bullet}$ to
520 generate 8-OhdG.[61] The increase in 8-OHdG in the cytoplasm implied that $OH^{\bullet}$
521 generated by QCT played an important role in DNA damage. It has been reported that
522 the *OGG1* gene product is responsible for removing 8-OHdG from DNA and to repair
523 damaged DNA.[62, 63] In the present study, QCT significantly affected the expression of
524 the *topo II*, *PCNA* and *Gadd45* genes; the influence of gene expression was
525 significantly decreased by SOD, indicating that ROS induced by QCT played a key
526 role in oxidative DNA damage.

527 In the previous studies, it was found that c-MYC-dependent activation of the
528 mitochondrial apoptotic pathway and tumor necrosis factor receptor (TNFR) pathway
529 may be associated with QCT-induced toxicity. [9, 64] The activation of c-MYC and
530 TNFR pathways could result in the activation of caspase-8 that cleaves effector
531 caspase-3 either directly or indirectly via the mitochondrial route. [64] Therefore, it was
532 suggested that the damage to mitochondria might play a critical role in the
533 genotoxicity of QCT. In the present study, mutations in mitochondrial DNA have
534 been noted in cells treated with QCT, suggesting that not only mitochondrial apoptotic
535 pathways but also mitochondrial DNA were affected by QCT.

536 Mitochondrial DNA is located in close proximity of the respiratory chain, which
537 is the main cellular source of ROS.[65] ROS can induce oxidative base lesions in
538 mitochondrial DNA, which might affect oxidative phosphorylation and result in
539 further ROS production.[66] Mutations in *ATP6*, *COX1 and COX3* have been noted in
540 cells treated with QCT. ATP6 is the ATP syntheses subunit 6 and participates the ATP

synthesis.[67] The mutation of ATP6 might affect ATP synthesis and result in disrupted ATP generation. ATP participates many kinds physiological functions, such as biosynthesis, energy transfer, metabolism and respiratory function.[68] If the synthesis of ATP is blocked, many kinds of physiological functions are affected, such as the respiratory chain, causing electron transport disruption and leading to the generation of ROS.[69] *COX3* is cytochrome c oxidase III which participates the composition of oxidase.[70] Mutations in the *COX3* gene might affect oxidase function, cause the electron transport disruption and result in electron leak, which is the resource of ROS. Thus, mutations in these genes in the mitochondrial DNA shed new light onto the mechanism of genotoxicity induced by QCT.

Topo II is highly enriched in the nuclear matrix and is responsible for resolving topological states that are encountered during replication and transcription.[71] Here, we showed that exposure to QCT inhibited topo II activity in nuclear extracts from HepG2 cells. Similarly, we found the same results regarding the reconnection skills of topoisomerase with pBR322 DNA. In the topo II catalytic cycle, enzyme binding to double-stranded DNA introduces a transient DNA DSB and passes the unbroken strand through the break. Topo II then religates the transient break and dissociated from the DNA. The topo II poison etoposide stabilizes the DNA-topo II complex and prevents religation, producing DNA DSBs.[72]

The TARDIS assay was first developed by Frank et al. to study melphalan adducts and modified by Willmore to detect DNA-topo II complexes.[73] The TARDIS assay shows that topo II is covalently bound to DNA in individual cells.[74] The present

563 results for the first time show that QCT can induce the HepG2 cells to form
564 DNA-topo II complexes and suggest that the inhibition of topo II activity was most
565 likely the result of the depletion of free topo II. ROS can attack enzymes and affect
566 their activity.[75] QCT could induce HepG2 cells to generate excessive ROS, which
567 might attack topoisomerase. In the present study, it was found that the inhibition of
568 topo II decreased by adding SOD, suggesting for the first time that ROS play a role in
569 the inhibition of topo II.

570 Genotoxic carcinogens such as polycyclic aromatic hydrocarbons (PAH) and
571 aflatoxin B1 (AFB1) are thought to cause cancer because of their ability to form
572 covalent bonds with DNA bases.[76, 77] The structures formed through the covalent
573 bonding of these intermediates to DNA bases are referred to as carcinogen-DNA
574 adducts.[78] Failure of the cell to repair these adducts can lead to mutations in the DNA
575 code.[79] We measured the interaction of DNA with QCT using ultraviolet absorption
576 spectrophotometry and HPLC. The results show that non-covalent binding between
577 DNA and QCT occurred. The non-covalent binding mode might be electrostatic or
578 groove binding, but not insert binding. The interaction of DNA with QCT might affect
579 the dissociation of topo II from the DNA and lead to a decrease in free topo II, which
580 would induce DNA strand breaks. In the present study, DSBs were generated after 2 h
581 of exposure to 20 μM QCT, and the degree of DNA strand breakage was most serious
582 after 4 h exposure to 40 μM QCT. However, the inhibition of topo II was greater at 20
583 μM than at 40 μM, indicating that a high dose of QCT exerts different genotoxic
584 mechanisms compared with those of a low dose of QCT. Further studies should be

carried out to investigate how a high dose of QCT exerts a toxic effect on topo II.

<Insert Fig. 8 here>

In summary, it was demonstrated for the first time that QCT caused DNA strand breaks and induced DNA damage by generating $O_2^{\bullet-}$ and $OH^{\bullet}$ during the metabolism process driven by XOR. After all defense systems were damaged, ROS could easily attack DNA and led to DNA strand breaks and mutations. QCT could induce the generation of topoisomerase-DNA complexes and affect DNA replication. These results provided valuable information on the mode and molecular mechanism of QCT toxicity.

Conflicts of interest

The authors have no conflicts of interest to report.

Acknowledgments

This work was supported by the Natural Science Foundation of China (31272614 and 31502115) and a grant from the National Basic Research Program of China (2009CB118800).

5 References

1. A. Carta, P. Corona and M. Loriga, *Current medicinal chemistry*, 2005, **12**, 2259-2272.
2. X. Wang, H. Zhang, L. Huang, Y. Pan, J. Li, D. Chen, G. Cheng, H. Hao, Y. Tao, Z. Liu and Z. Yuan, *Chem. Res. Toxicol.*, 2015, **28**, 470-481.
3. Y. Wu, Y. Wang, L. Huang, Y. Tao, Z. Yuan and D. Chen, *Anal. Chim. Acta*, 2006, **569**, 97-102.
4. A. Ihsan, X. Wang, Z. Liu, Y. Wang, X. Huang, Y. Liu, H. Yu, H. Zhang, T. Li and C. Yang, *Toxicol. Appl. Pharmacol.*, 2011, **252**, 281-288.
5. A. Ihsan, X. Wang, H. G. Tu, W. Zhang, M. H. Dai, D. P. Peng, Y. L. Wang, L. L. Huang, D. M. Chen, S. Mannan, Y. F. Tao, Z. L. Liu and Z. H. Yuan, *Food Chem. Toxicol.*, 2013, **51**, 330-336.
6. A. Ihsan, X. Wang, W. Zhang, H. Tu, Y. Wang, L. Huang, Z. Iqbal, G. Cheng, Y. Pan, Z. Liu, Z. Tan, Y. Zhang and Z. Yuan, *Food Chem. Toxicol.*, 2013, **59C**, 207-214.
7. J. Liu, M. Ouyang, J. Jiang, P. Mu, J. Wu, Q. Yang, C. Zhang, W. Xu, L. Wang, M. S. Huen and Y. Deng, *Mutat. Res.*, 2012, **741**, 70-75.
8. K. Zhang, X. Wang, C. Wang, H. Zheng, T. Li, S. Xiao, M. Wang, C. Fei, L. Zhang and F. Xue, *Environ. Toxicol. Pharmacol.*, 2015, **39**, 555-567.
9. K. Zhang, W. Zheng, H. Zheng, C. Wang, M. Wang, T. Li, X. Wang, L. Zhang, S. Xiao, C. Fei and F. Xue, *Cell Biol. Toxicol.*, 2014, **30**, 313-329.
10. W. Yang, J. Fu, X. Xiao, H. Yan, W. Bao, D. Wang, L. Hao, A. K. Nussler, P. Yao and L. Liu, *J. Sci. Food Agric.*, 2012.
11. M. Yu, D. Wang, M. Xu, Y. Liu, X. Wang, J. Liu, X. Yang, P. Yao, H. Yan and L. Liu, *Food Chem. Toxicol.*, 2014, **69**, 210-219.

12. J. Zou, Q. Chen, S. Tang, X. Jin, K. Chen, T. Zhang and X. Xiao, *Mutation Research/Genetic Toxicology and Environmental Mutagenesis*, 2009, **676**, 27-33.

13. X.-J. Huang, H.-H. Zhang, X. Wang, L.-L. Huang, L.-Y. Zhang, C.-X. Yan, Y. Liu and Z.-H. Yuan, *Chem.-Biol. Interact.*, 2010, **185**, 227-234.

14. D. Wang, Y. Zhong, X. Luo, S. Wu, R. Xiao, W. Bao, W. Yang, H. Yan, P. Yao and L. Liu, *Food and Chemical Toxicology*, 2011, **49**, 477-484.

15. T. B. Kryston, A. B. Georgiev, P. Pissis and A. G. Georgakilas, *Mutation Research/Fundamental and Molecular Mechanisms of Mutagenesis*, 2011, **711**, 193-201.

16. W. X. Li, L. P. Chen, Y. W. Su, H. Yin, Y. Q. Pang and Z. X. Zhuang, *Toxicol Res-Uk*, 2015, **4**, 1389-1399.

17. S. L. Zhuang, L. L. Bao, H. F. Wang, M. Zhang, C. Yang, X. Y. Zhou, Y. Wu, K. Rehman and H. Naranmandura, *Toxicol Res-Uk*, 2015, **4**, 1195-1203.

18. M. S. Cooke, M. D. Evans, M. Dizdaroglu and J. Lunec, *The FASEB Journal*, 2003, **17**, 1195-1214.

19. A. M. Falchi, A. Rosa, A. Atzeri, A. Incani, S. Lampis, V. Meli, C. Caltagirone and S. Murgia, *Toxicol Res-Uk*, 2015, **4**, 1025-1036.

20. I. Pujalte, I. Passagne, R. Daculsi, C. de Portal, C. Ohayon-Courtes and B. L'Azou, *Toxicol Res-Uk*, 2015, **4**, 409-422.

21. F. A. B. da Cunha, G. L. Wallau, A. I. Pinho, M. E. M. Nunes, N. F. Leite, S. R. Tintino, G. M. da Costa, M. L. Athayde, A. A. Boligon, H. D. M. Coutinho, A. B. Pereira, T. Posser and J. L. Franco, *Toxicol Res-Uk*, 2015, **4**, 634-644.

22. M. Valko, M. Izakovic, M. Mazur, C. J. Rhodes and J. Telser, *Mol. Cell. Biochem.*, 2004, **266**,

37-56.

23. T. Devasagayam, J. Tilak, K. Boloor, K. Sane, S. Ghaskadbi and R. Lele, *Japi*, 2004, **52**, 794-804.

24. M. H. Moustafa, R. K. Sharma, J. Thornton, E. Mascha, M. A. Abdel‐Hafez, A. J. Thomas and A. Agarwal, *Hum. Reprod.*, 2004, **19**, 129-138.

25. A. K. Larsen, A. E. Escargueil and A. Skladanowski, *Pharmacol. Ther.*, 2003, **99**, 167-181.

26. A. R. Chaudhuri, Y. Hashimoto, R. Herrador, K. J. Neelsen, D. Fachinetti, R. Bermejo, A. Cocito, V. Costanzo and M. Lopes, *Nat. Struct. Mol. Biol.*, 2012, **19**, 417-423.

27. K. B. Peters and J. M. Brown, *Cancer Res.*, 2002, **62**, 5248-5253.

28. J. B. Ward Jr and R. E. Henderson, *Environ. Health Perspect.*, 1996, **104**, 895.

29. B. Hang, *Journal of nucleic acids*, 2010, **2010**.

30. G. Xiao, A. Chicas, M. Olivier, Y. Taya, S. Tyagi, F. R. Kramer and J. Bargonetti, *Cancer Res.*, 2000, **60**, 1711-1719.

31. M. G. Kemp, L. A. Lindsey-Boltz and A. Sancar, *J. Biol. Chem.*, 2011, **286**, 19237-19246.

32. M. Wu, W. Che and Z. Zhang, *Environ. Mol. Mutagen.*, 2008, **49**, 265-275.

33. C.-X. Deng, *Nucleic Acids Res.*, 2006, **34**, 1416-1426.

34. T. K. Hazra, A. Das, S. Das, S. Choudhury, Y. W. Kow and R. Roy, *DNA Repair*, 2007, **6**, 470-480.

35. K. Zhang, M. Ban, Z. Zhao, H. Zheng, X. Wang, M. Wang, C. Fei and F. Xue, *Research in Veterinary Science*, 2012.

36. Q. Chen, S. Tang, X. Jin, J. Zou, K. Chen, T. Zhang and X. Xiao, *Food Chem. Toxicol.*, 2009, **47**, 328-334.

37. M. M. Ismail, K. M. Amin, E. Noaman, D. H. Soliman and Y. A. Ammar, *Eur. J. Med. Chem.*,

2010, **45**, 2733-2738.

38. B. Ganley, G. Chowdhury, J. Bhansali, J. S. Daniels and K. S. Gates, *Biorg. Med. Chem.*, 2001, **9**, 2395-2401.

39. L. Hao, Q. Chen and X. Xiao, *Mutat. Res.*, 2006, **599**, 21-25.

40. B. Singh and H. K. Bhat, *Carcinogenesis*, 2012, **33**, 2601-2610.

41. N. Shahabadi and L. Heidari, *Spectrochim. Acta. A Mol. Biomol. Spectrosc.*, 2012, **97**, 406-410.

42. C. Y. Chen, M. H. Ma, Z. H. Zhou, K. Lu and B. R. Xiang, *Guang pu xue yu guang pu fen xi = Guang pu*, 2006, **26**, 1891-1894.

43. E. Eruslanov and S. Kusmartsev, in *Advanced Protocols in Oxidative Stress II*, Springer, 2010, pp. 57-72.

44. H. M. Peshavariya, G. J. Dusting and S. Selemidis, *Free Radic. Res.*, 2007, **41**, 699-712.

45. E. Willmore, A. Frank, K. Padget, M. Tilby and C. Austin, *Mol. Pharmacol.*, 1998, **54**, 78-85.

46. A. Chakraborty, M. Sakai and Y. Iwatsuki, *J. Appl. Ichthyol.*, 2006, **22**, 160-166.

47. T. D. Schmittgen and K. J. Livak, *Nat. Protoc.*, 2008, **3**, 1101-1108.

48. X. Wang, Q. Liu, A. Ihsan, L. Huang, M. Dai, H. Hao, G. Cheng, Z. Liu, Y. Wang and Z. Yuan, *Toxicol. Sci.*, 2012, **127**, 412-424.

49. B. Hong, V. W. Lui, E. P. Hui, M. H. Ng, S. H. Cheng, F. L. Sung, C. M. Tsang, S. W. Tsao and A. T. Chan, *Invest. New Drugs*, 2011, **29**, 401-410.

50. K. Ghattass, S. El-Sitt, K. Zibara, S. Rayes, M. J. Haddadin, M. El-Sabban and H. Gali-Muhtasib, *Mol. Cancer*, 2014, **13**, 12.

51. X. Jin, Q. Chen, S. S. Tang, J. J. Zou, K. P. Chen, T. Zhang and X. L. Xiao, *Toxicol. In Vitro*, 2009, **23**, 1209-1214.

52. X. Wang, X. J. Huang, A. Ihsan, Z. Y. Liu, L. L. Huang, H. H. Zhang, H. F. Zhang, W. Zhou, Q. Liu, X. J. Xue and Z. H. Yuan, *Toxicology*, 2011, **280**, 126-134.

53. K. Zhang, M. Ban, Z. Zhao, H. Zheng, X. Wang, M. Wang, C. Fei and F. Xue, *Res. Vet. Sci.*, 2012, **93**, 1393-1401.

54. B. Brodská and A. Holoubek, *Oxid. Med. Cell. Longev.*, 2011, **2011**.

55. L. L. Wu, C.-C. Chiou, P.-Y. Chang and J. T. Wu, *Clin. Chim. Acta*, 2004, **339**, 1-9.

56. J. L. Wei, L. S. Zhang, J. J. Wang, F. Z. Guo, Y. B. Li, X. Q. Zhou and Z. W. Sun, *Toxicol Res-Uk*, 2015, **4**, 1282-1288.

57. Y.-Z. Fang, S. Yang and G. Wu, *Nutrition*, 2002, **18**, 872-879.

58. R. Sharma, H. Eng, G. S. Walker, G. Barreiro, A. F. Stepan, K. F. McClure, A. Wolford, P. D. Bonin, P. Cornelius and A. S. Kalgutkar, *Chem. Res. Toxicol.*, 2011, **24**, 2207-2216.

59. Z. Liu and Z. Sun, *Medicinal chemistry (Shariqah (United Arab Emirates))*, 2013, **9**, 1017-1027.

60. C. E. Berry and J. M. Hare, *The Journal of physiology*, 2004, **555**, 589-606.

61. A. Kumar, V. Pottiboyina and M. D. Sevilla, *The Journal of Physical Chemistry B*, 2011, **115**, 15129-15137.

62. A. Azqueta, L. Arbillaga, G. Pachón, M. Cascante, E. E. Creppy and A. L. d. Cerain, *Chem.-Biol. Interact.*, 2007, **168**, 95-105.

63. B. Karahalil, E. Kesimci, E. Emerce, T. Gumus and O. Kanbak, *Mol. Biol. Rep.*, 2011, **38**, 2427-2435.

64. C. Zhang, C. Wang, S. Tang, Y. Sun, D. Zhao, S. Zhang, S. Deng, Y. Zhou and X. Xiao, *Food Chem. Toxicol.*, 2013, **62**, 825-838.

65. K. Ishikawa, K. Takenaga, M. Akimoto, N. Koshikawa, A. Yamaguchi, H. Imanishi, K. Nakada, Y.

Honma and J.-I. Hayashi, *Science*, 2008, **320**, 661-664.

66. M. D. Brand, C. Affourtit, T. C. Esteves, K. Green, A. J. Lambert, S. Miwa, J. L. Pakay and N. Parker, *Free Radic. Biol. Med.*, 2004, **37**, 755-767.

67. P. Cortés-Hernández, M. E. Vázquez-Memije and J. J. García, *J. Biol. Chem.*, 2007, **282**, 1051-1058.

68. G. Barja, *Rejuvenation research*, 2007, **10**, 215-224.

69. J. St-Pierre, J. A. Buckingham, S. J. Roebuck and M. D. Brand, *J. Biol. Chem.*, 2002, **277**, 44784-44790.

70. F. Xu, C. Morin, G. Mitchell, C. Ackerley and B. Robinson, *Biochem. J*, 2004, **382**, 331-336.

71. Y. L. Lyu, C.-P. Lin, A. M. Azarova, L. Cai, J. C. Wang and L. F. Liu, *Mol. Cell. Biol.*, 2006, **26**, 7929-7941.

72. D. A. Jacob, S. L. Mercer, N. Osheroff and J. E. Deweese, *Biochemistry*, 2011, **50**, 5660-5667.

73. J. Rothbarth, C. Koevoets, R. A. Tollenaar, M. J. Tilby, C. J. van de Velde, G. J. Mulder and P. J. Kuppen, *Biochem. Pharmacol.*, 2004, **67**, 1771-1778.

74. O. Cuvier, S. Stanojcic, J.-M. Lemaitre and M. Mechali, *Genes Dev.*, 2008, **22**, 860-865.

75. S. J. S. Flora, N. Dwivedi, U. Deb, P. Kushwaha and V. Lomash, *Toxicol Res-Uk*, 2014, **3**, 23-31.

76. B. P. Cho, *Journal of Environmental Science and Health, Part C*, 2004, **22**, 57-90.

77. S. R. Myers, M. Y. Ali, T. Wright and C. Cunningham, *Polycyc. Aromatic Compounds*, 2007, **27**, 339-359.

78. J. C. Delaney and J. M. Essigmann, *Chem. Res. Toxicol.*, 2007, **21**, 232-252.

79. K. Kropachev, M. Kolbanovskiy, Z. Liu, Y. Cai, L. Zhang, A. G. Schwaid, A. Kolbanovskiy, S. Ding, S. Amin and S. Broyde, *Chem. Res. Toxicol.*, 2013, **26**, 783-793.

735 **Figure legends**

736 **Fig. 1** The chemical structures of QdNOs and their metabolites.

737

738 **Fig. 2** DNA strand break induction by quinoxalines in V79 cells and HepG2 cells.
739 Cells were incubated with the drug at the tested concentration of 40 μM for 4 h. (A)
740 DNA strand break was determined by the SCGE assay. The OTM of HepG2 cells and
741 V79 cells treated with QdNOs was assessed. (B) The OTM of HepG2 cells treated
742 with QdNOs and their metabolites at 40 μM for 4 h, and the OTM of HepG2 cells
743 treated with 0, 10, 20, 30 and 40 μM QCT for 1, 2 and 4 h, respectively. Data shown
744 means ± SD (n = 3). *$P < 0.05$ and **$P < 0.01$ vs. the blank control group.

745 *Notes*: CBX, carbadox; CY1, N1-deoxy cyadox; CY2, N4-deoxy cyadox; CY5,
746 bi-deoxy cyadox; CY9, quinoxaline-2-carboxylic acid; CYA, cyadox; H_2O_2, peroxide;
747 M1, 2-isoethanol mequindox; M2, 2-isoethanol 1-desoxymequindox; M4, bi-desoxy
748 mequindox; M10, 2-isoethanol bi-desoxymequindox; MEQ, mequindox; MQCA,
749 3-methyl-quinoxaline-2-carboxylic acid; OLA, olaquindox; Q4, N1-deoxy
750 quinocetone; Q5, N4-deoxy quinocetone; Q6, bi-deoxy quinocetone; Q7,
751 3-methyl-2-quinoxalinebenzenevinylalcohol; QCT, quinocetone.

752

753 **Fig. 3** Ultraviolet absorption spectroscopy of ct-DNA upon the addition of
754 quinocetone (QCT) (A) and HPLC diagram of dinucleotide (12.5 mg/mL) with 40 μM
755 of QCT (B, C, D, E, F, G, H, I and J). (A) The interaction of ct-DNA with QCT was

exposed at 37 °C, for 4 h. From a to g: 200 μM DNA+40 μM QCT, 100 μM DNA+40 μM QCT, 50 μM DNA+40 μM QCT, 200 μM DNA, 25 μM DNA+40 μM QCT, 12.5 μM DNA+40 μM QCT, and 40 μM QCT. (B) QCT. (C) dAMP. (D) dTMP. (E) dCMP. (F) dGMP. (G) dAMP + QCT. (H) dTMP + QCT. (I) dCMP + QCT; (J) dGMP + QCT.

Fig. 4 The generation of ROS, $O_2^{\bullet-}$ and metabolites in HepG2 cells induced by quinocetone (QCT). (A) HepG2 cells were treated with various concentrations of QCT (0-40 μM) for 0.5, 1, 2, 3 and 4 h. Total ROS generation induced by QCT was expressed as relative fluorescence units in the DCFH assay. (B) $O_2^{\bullet-}$ generation in HepG2 cells was induced by 0-40 μM QCT for 0.5-4 h. (C) $O_2^{\bullet-}$ generation by QCT (10-160 μM) occurred in the process of metabolism with XOR (50 μM) for 0.5 h. (D) The influence of $O_2^{\bullet-}$ generation by the treatment of SOD. (E) The generation of 8-OHdG in HepG2 cells with QCT treatment for 4 h. (F) The comparison of $O_2^{\bullet-}$ generation by QCT and bi-deoxy quinocetone (Q6) when cells were treated for 4 h. (G) The generation of N4-deoxy quinocetone (Q3), N1-deoxy quinocetone (Q4) and bidesoxy-quinocetone (Q6) when QCT was incubated with HepG2 cells. (H) QCT incubated with cell culture medium. Data are means ± SD (n = 3). *$P < 0.05$ and **$P < 0.01$ vs. the blank control group; # $P < 0.05$ vs. the same dose in the QCT group.

Fig. 5 Cleavage of supercoiled plasmid DNA (pBR322 DNA) by quinocetone (QCT) in the presence of xanthine/xanthine oxidase (X/XOR) as an activating system. The reactions contain DNA (50 μg/mL), sodium phosphate buffer (50 mM, pH 7.0),

778 xanthine (100 μM), XOR (8.75 U/mL), QCT (160 μM), TPZ (500 μM) and SOD
779 (3.25 U/μL) were prepared and incubated under aerobic (A) and low oxygen
780 conditions (B). After incubation for 2 h at 37 °C, the reactions were analyzed by
781 agarose gel electrophoresis. (A) 1, pBR32 DNA; 2, DNA+X/XOR; 3,
782 DNA+X/XOR+TPZ; 4, DNA+X/XOR+QCT; 5, DNA+X/XOR+QCT+DMSO; 6,
783 DNA+X/XOR+QCT+SOD; 7, DNA+X/XOR+SOD; 8, DNA+X/XOR+DMSO; 9,
784 DNA+X/XOR+TPZ+SOD; 10, DNA+X/XOR+TPZ+DMSO. (B) a, pBR322 DNA; b,
785 DNA+X/XOR; c, DNA+X/XOR+SOD; d, DNA+X/XOR+DMSO; e,
786 DNA+X/XOR+TPZ; f, DNA+X/XOR+TPZ+DMSO; g, DNA+X/XOR+QCT; h,
787 DNA+X/XOR+QCT+DMSO; i, DNA+QCT; j: DNA+X/XOR+QCT+SOD.
788
789 **Fig. 6** Inhibition of topo I and topo II activity induced by QCT. (A) Inhibition of topo
790 I activity *in vitro* by QCT. Line 1, pBR322 DNA; Line 2, topo II+pBR322 DNA; Line
791 3, topo I+pBR322 DNA+40 μM QCT; Line 4, topo I+pBR322 DNA+80 μM QCT;
792 Line 5, topo I+pBR322 DNA+160 μM QCT; Line 6, topo I+pBR322 DNA+100 μM
793 VP-16. (B) Inhibition of topo II activity *in vitro* by QCT. Line 1, pBR322 DNA; Line
794 2, topo II+pBR322 DNA; Line 3, topo II+pBR322 DNA+20 μM QCT; Line 4, topo
795 II+pBR322 DNA+40 μM QCT; Line 5, topo II+pBR322 DNA+80 μM QCT; Line 6,
796 topo II+pBR322 DNA+100 μM VP-16. (C) Generation of DNA-topo II complexes of
797 HepG2 cells induced by QCT. HepG2 cells were treated with 40 μM QCT for 4 h.
798 After treatment, cells were suspended in agarose gels on glass slides, lysed and probed
799 with anti-topo II antibodies. Anti-topo II binding was visualized with secondary

antibody conjugated to FITC. Left panels, DAPI-stained DNA; right panels, fluorescein-stained topo II.

Fig. 7 Level of expression of DNA replication and repair genes in HepG2 cells treated with various concentrations of quinocetone (QCT). (A) Cells treated with QCT at 10, 20, 30 and 40 μM for 4 h. (B) Cells treated with QCT at 40 μM and 3.25 U/μL SOD for different exposure times. Data are means ± SD (n = 3). *$P < 0.05$ and **$P < 0.01$ vs. the blank control group; # $P < 0.05$ vs. the same dose in the QCT group.

Fig. 8 The proposed mechanisms of the genotoxicity of quinocetone (QCT). The production of $O_2^{\bullet-}$ and $OH^{\bullet}$ occurs via the reduction of the N-O group of QCT. After all defense systems are damaged, ROS can easily attack the mitochondrial DNA and cause gene mutations. Furthermore, QCT can also induce the generation of topoisomerase-DNA complexes and affect DNA replication.

821 **Table 1** Primer sequence of mtDNA

Gene	Sequence (5'-3')	Length (bps)
D-loop	Fwd: GCATTTGGTATTTTCGCTTGGGG	795
	Rev: CTATTGACTTGGGTTAATCGTGT	
rRNA1	Fwd: ACACCCCCACGGGAAACAGCAGT	936
	Rev: TGGGTAAATGGTTTGGCTAAGGT	
tRNA1	Fwd: CCACCTTACTACCAGACAACCTT	774
	Rev: TTTTTGGTAAACAGGCGGGGTAA	
rRNA2	Fwd: AGGAACTCGGCAAATCTTACCCC	732
	Rev: GGAATTGAACCTCTGACTGTAAA	
tRNA2	Fwd: CACCCTCACCACTACAATCTTCC	798
	Rev: GGGCTAGTTTTTGTCATGTGAGA	
tRNA3	Fwd: GCTAAGCCCTTACTAGACCAATG	858
	Rev: TGGGAGAGATAGGAGAAGTAGGA	
COX1	Fwd: TGCCATAACCCAATACCAAACGC	912
	Rev: GGTTTATGGAGGGTTCTTCTACT	
ATP6	Fwd: CTTGACGTTGACAATCGAGTAGT	890
	Rev: AGCGAAAGCCTATAATCACTGCG	
COX3	Fwd: TGCCTCACTCATTTACACCAACC	892
	Rev: TTTGGTTTCGGTTGTTTTCTATT	
ND3	Fwd: ACAAAAAGGATTAGACTGAGCCG	936

Gene	Sequence (5'-3')	Length (bps)
	Rev: GTTCTTGGGCAGTGAGGGTGAGT	
ND4	Fwd: GGCTCCCTTCCCCTACTCATCGC	1010
	Rev: ATGAGTTAGCAGTTCTTGTGAGC	

Note: *ATP6*, ATP synthase F0 subunit 6; *COX1* (cytochrome c oxidase I); *COX3* (cytochrome c oxidase II); *ND3* (NADH dehydrogenease subit 3); *ND4* (NADH dehydrogenease subit 4); *rRNA1* (12s ribosomal RNA); *rRNA2* (16s ribosomal RNA); *tRNA1* (tRNA-Lys); *tRNA2* (tRNA-Ser); *tRNA3* (tRNA-Leu).

839 **Table 2** Primer Used for the qRT-PCR Analysis

Gene	Sequence (5'–3')	Length (bps)
GAPDH	Fwd: GCCCAAGATGCCCTTCAGT	160
	Rev: CCTTCCGTGTTCCTACCCC	
Gadd45	Fwd: AGCAGAAGACCGAAAGCG	106
	Rev: TGGATCAGGGTGAAGTGGA	
RAD50	Fwd: CCTGTGGCGAAGTACCTAT	138
	Rev: CTGGAAGTTACGCTGCTGT	
RAD51	Fwd: TAAAGCAGAAGCCTTAGAAAC	138
	Rev: TTATGAAGCCCTGGGTATG	
RFC	Fwd: AGCAAGGCTAGGAATTTGG	290
	Rev: AGGGAAGCTGTGGTGGTT	
DNA-PK	Fwd: AAGAAAGGTCAAACAAGAG	151
	Rev: CGAGGGAGTTAGTCCAAAGA	
OGG1	Fwd: CTGGACCTGGTTCTGCCTTC	366
	Rev: AGTGATGCGGGCGATGTTGT	
BRCA1	Fwd: CTTGAGGACCTGCGAAAT	217
	Rev: GCATGTACCACCTATCATCT	
CDC6	Fwd: CGCAAAGCACTGGATGTT	153
	Rev: GATGACTTGGGATATGTGAAT	
POLB	Fwd: AATCACCGACATGCTCACA	285

Gene	Sequence (5'–3')	Length (bps)
	Rev: GATGGACCAATGCCACTAAC	
RPA3	Fwd: TCGAGTTGATGGAACCCCTT	208
	Rev: CAATCATGTTGCACAATCCCT	
topo II	Fwd: TTCTAGTTAATGCTGCGGACA	237
	Rev: CTCCATAGCCATTTCGACCA	
PCNA	Fwd: CAAGGACCTCATCAACGA	227
	Rev: TATCTTCGGCCCTTAGTGT	

840 *Note*. Primers were manufactured by Shanghai Generay Biotech Co., Ltd
841 (Shanghai, PR China).
842
843
844
845
846
847
848
849
850
851
852

853 **Table 3** Sequence of mitochondrial DNA after treatment with quinocetone

Mutation site	Gene	Blank sequence	Mutation sequence	Codon changes
6488	*COX1*	TAC*TT*CTCCT	TAC*TTT*CTCCT	Insertion
8849	*ATP6*	CCCTTATGAG	CCC*TTT*ATGAG	Insertion
9744	*COX3*	CTC*AGA*GTAC	CTC*AAA*GTAC	GAG>AAG

854
855
856
857
858
859
860
861
862
863
864
865
866
867
868
869
870
871
872
873
874
875

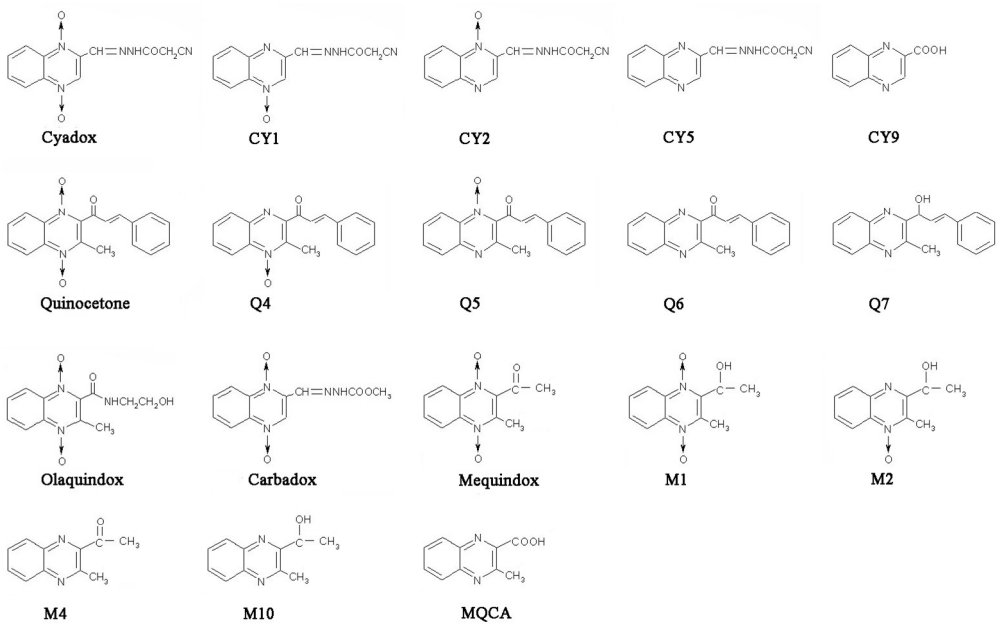

Fig. 1 The chemical structures of QdNOs and their metabolites.
131x82mm (300 x 300 DPI)

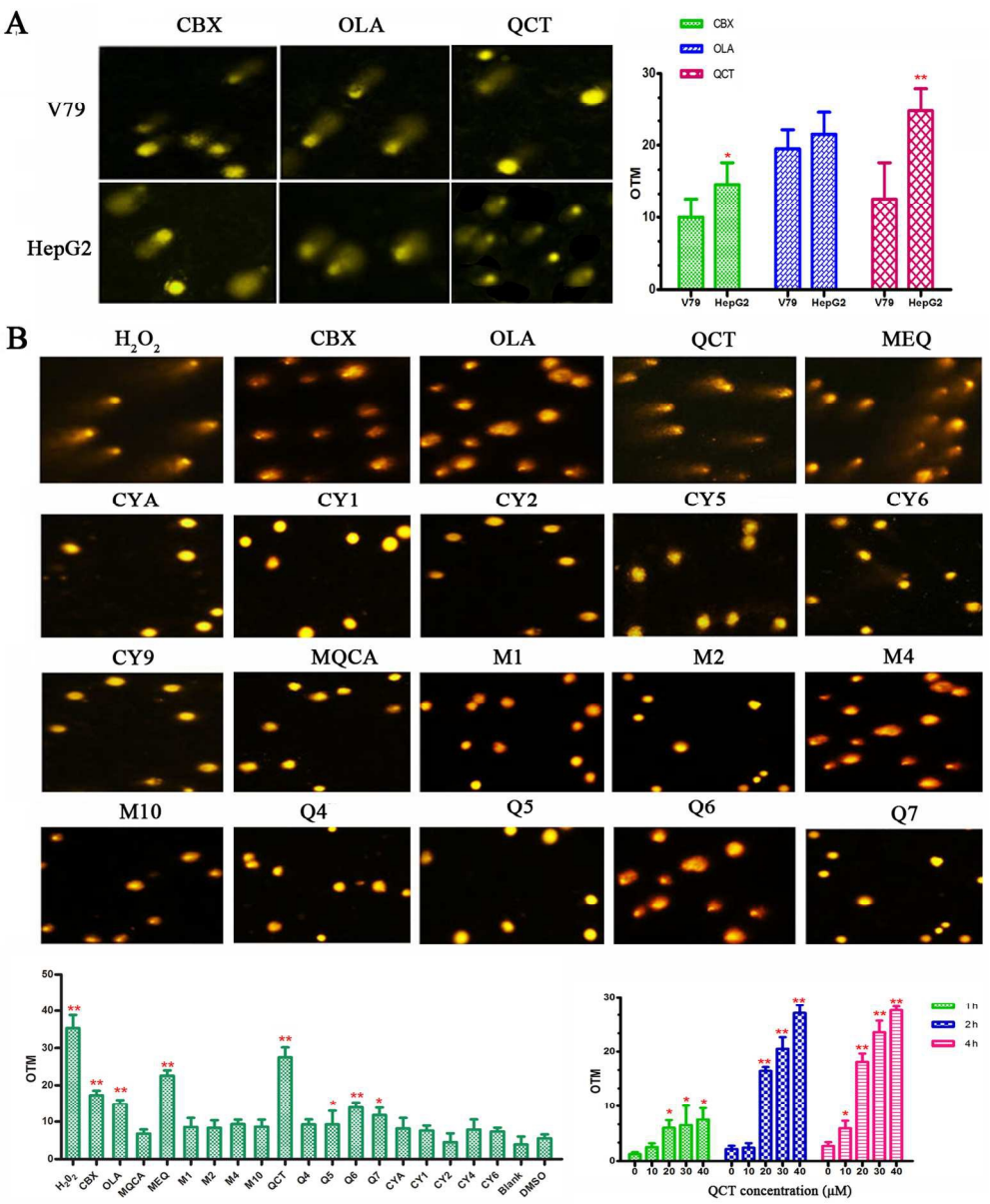

Fig. 2 DNA strand break induction by quinoxalines in V79 cells and HepG2 cells. Cells were incubated with the drug at the tested concentration of 40 μM for 4 h. (A) DNA strand break was determined by the SCGE assay. The OTM of HepG2 cells and V79 cells treated with QdNOs was assessed. (B) The OTM of HepG2 cells treated with QdNOs and their metabolites at 40 μM for 4 h, and the OTM of HepG2 cells treated with 0, 10, 20, 30 and 40 μM QCT for 1, 2 and 4 h, respectively. Data shown means ± SD (n = 3). *P < 0.05 and **P < 0.01 vs. the blank control group.
128x156mm (300 x 300 DPI)

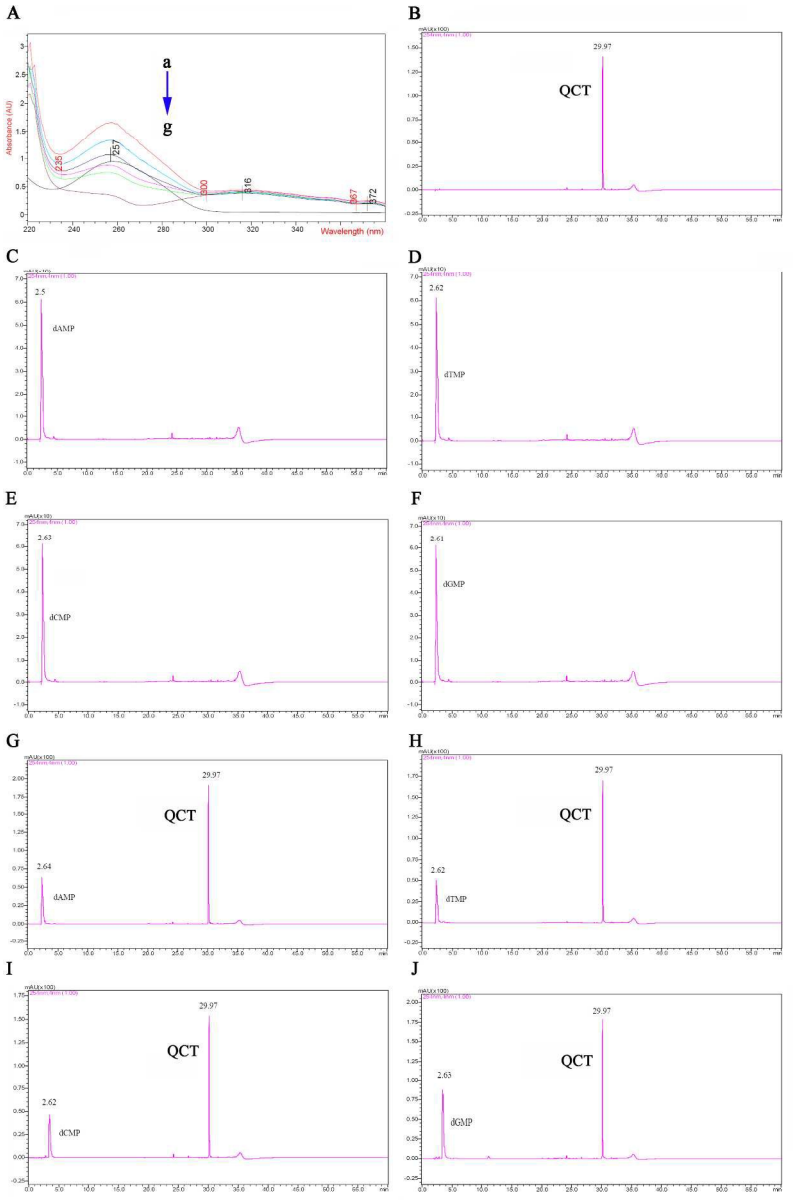

Fig. 3 Ultraviolet absorption spectroscopy of ct-DNA upon the addition of quinocetone (QCT) (A) and HPLC diagram of dinucleotide (12.5 mg/mL) with 40 μM of QCT (B, C, D, E, F, G, H, I and J). (A) The interaction of ct-DNA with QCT was exposed at 37 °C, for 4 h. From a to g: 200 μM DNA+40 μM QCT, 100 μM DNA+40 μM QCT, 50 μM DNA+40 μM QCT, 200 μM DNA, 25 μM DNA+40 μM QCT, 12.5 μM DNA+40 μM QCT, and 40 μM QCT. (B) QCT. (C) dAMP. (D) dTMP. (E) dCMP. (F) dGMP. (G) dAMP + QCT. (H) dTMP + QCT. (I) dCMP + QCT; (J) dGMP + QCT.
181x275mm (300 x 300 DPI)

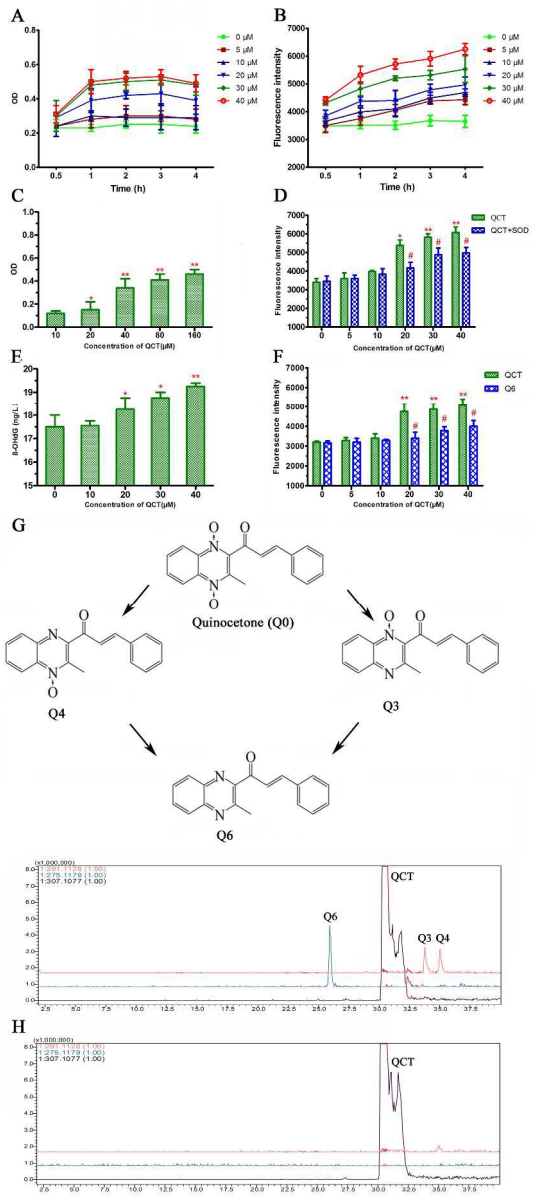

Fig. 4 The generation of ROS, O2•- and metabolites in HepG2 cells induced by quinocetone (QCT). (A) HepG2 cells were treated with various concentrations of QCT (0-40 μM) for 0.5, 1, 2, 3 and 4 h. Total ROS generation induced by QCT was expressed as relative fluorescence units in the DCFH assay. (B) O2•- generation in HepG2 cells was induced by 0-40 μM QCT for 0.5-4 h. (C) O2•- generation by QCT (10-160 μM) occurred in the process of metabolism with XOR (50 μM) for 0.5 h. (D) The influence of O2•- generation by the treatment of SOD. (E) The generation of 8-OHdG in HepG2 cells with QCT treatment for 4 h. (F) The comparison of O2•- generation by QCT and bi-deoxy quinocetone (Q6) when cells were treated for 4 h. (G) The generation of N4-deoxy quinocetone (Q3), N1-deoxy quinocetone (Q4) and bidesoxy-quinocetone (Q6) when QCT was incubated with HepG2 cells. (H) QCT incubated with cell culture medium. Data are means ± SD (n = 3). *P < 0.05 and **P < 0.01 vs. the blank control group; # P < 0.05 vs. the same dose in the QCT group.

168x383mm (300 x 300 DPI)

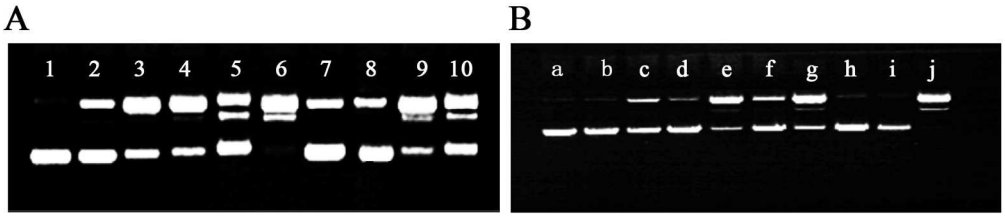

Fig. 5 Cleavage of supercoiled plasmid DNA (pBR322 DNA) by quinocetone (QCT) in the presence of xanthine/xanthine oxidase (X/XOR) as an activating system. The reactions contain DNA (50 μg/mL), sodium phosphate buffer (50 mM, pH 7.0), xanthine (100 μM), XOR (8.75 U/mL), QCT (160 μM), TPZ (500 μM) and SOD (3.25 U/μL) were prepared and incubated under aerobic (A) and low oxygen conditions (B). After incubation for 2 h at 37 °C, the reactions were analyzed by agarose gel electrophoresis. (A) 1, pBR32 DNA; 2, DNA+X/XOR; 3, DNA+X/XOR+TPZ; 4, DNA+X/XOR+QCT; 5, DNA+X/XOR+QCT+DMSO; 6, DNA+X/XOR+QCT+SOD; 7, DNA+X/XOR+SOD; 8, DNA+X/XOR+DMSO; 9, DNA+X/XOR+TPZ+SOD; 10, DNA+X/XOR+TPZ+DMSO. (B) a, pBR322 DNA; b, DNA+X/XOR; c, DNA+X/XOR+SOD; d, DNA+X/XOR+DMSO; e, DNA+X/XOR+TPZ; f, DNA+X/XOR+TPZ+DMSO; g, DNA+X/XOR+QCT; h, DNA+X/XOR+QCT+DMSO; i, DNA+QCT; j: DNA+X/XOR+QCT+SOD.
180x38mm (300 x 300 DPI)

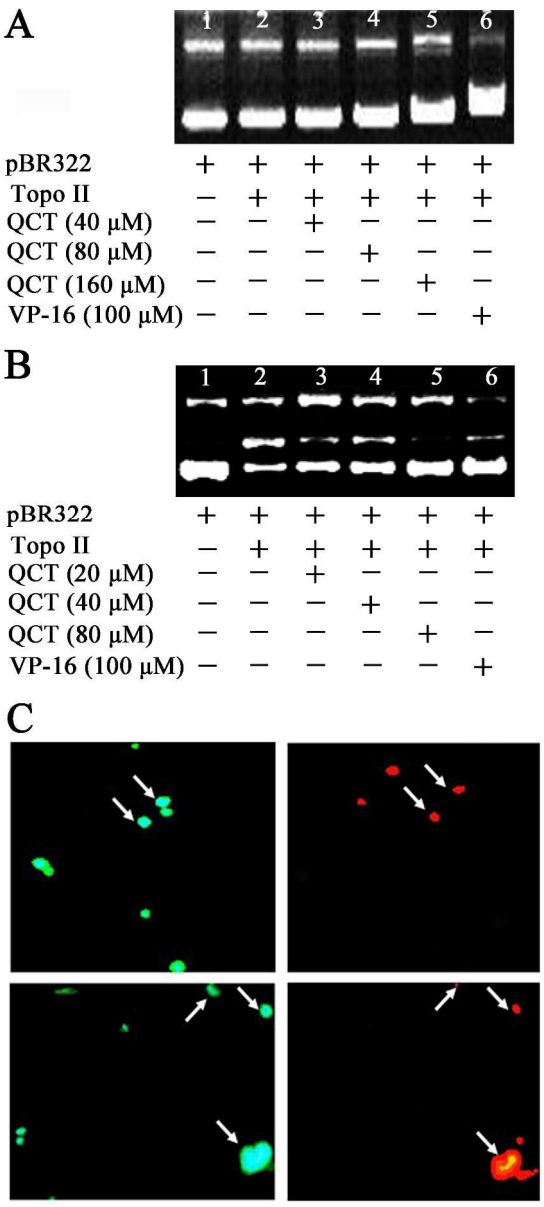

Fig. 6 Inhibition of topo I and topo II activity induced by QCT. (A) Inhibition of topo I activity in vitro by QCT. Line 1, pBR322 DNA; Line 2, topo II+pBR322 DNA; Line 3, topo I+pBR322 DNA+40 μM QCT; Line 4, topo I+pBR322 DNA+80 μM QCT; Line 5, topo I+pBR322 DNA+160 μM QCT; Line 6, topo I+pBR322 DNA+100 μM VP-16. (B) Inhibition of topo II activity in vitro by QCT. Line 1, pBR322 DNA; Line 2, topo II+pBR322 DNA; Line 3, topo II+pBR322 DNA+20 μM QCT; Line 4, topo II+pBR322 DNA+40 μM QCT; Line 5, topo II+pBR322 DNA+80 μM QCT; Line 6, topo II+pBR322 DNA+100 μM VP-16. (C) Generation of DNA-topo II complexes of HepG2 cells induced by QCT. HepG2 cells were treated with 40 μM QCT for 4 h. After treatment, cells were suspended in agarose gels on glass slides, lysed and probed with anti-topo II antibodies. Anti-topo II binding was visualized with secondary antibody conjugated to FITC. Left panels, DAPI-stained DNA; right panels, fluorescein-stained topo II.
139x307mm (300 x 300 DPI)

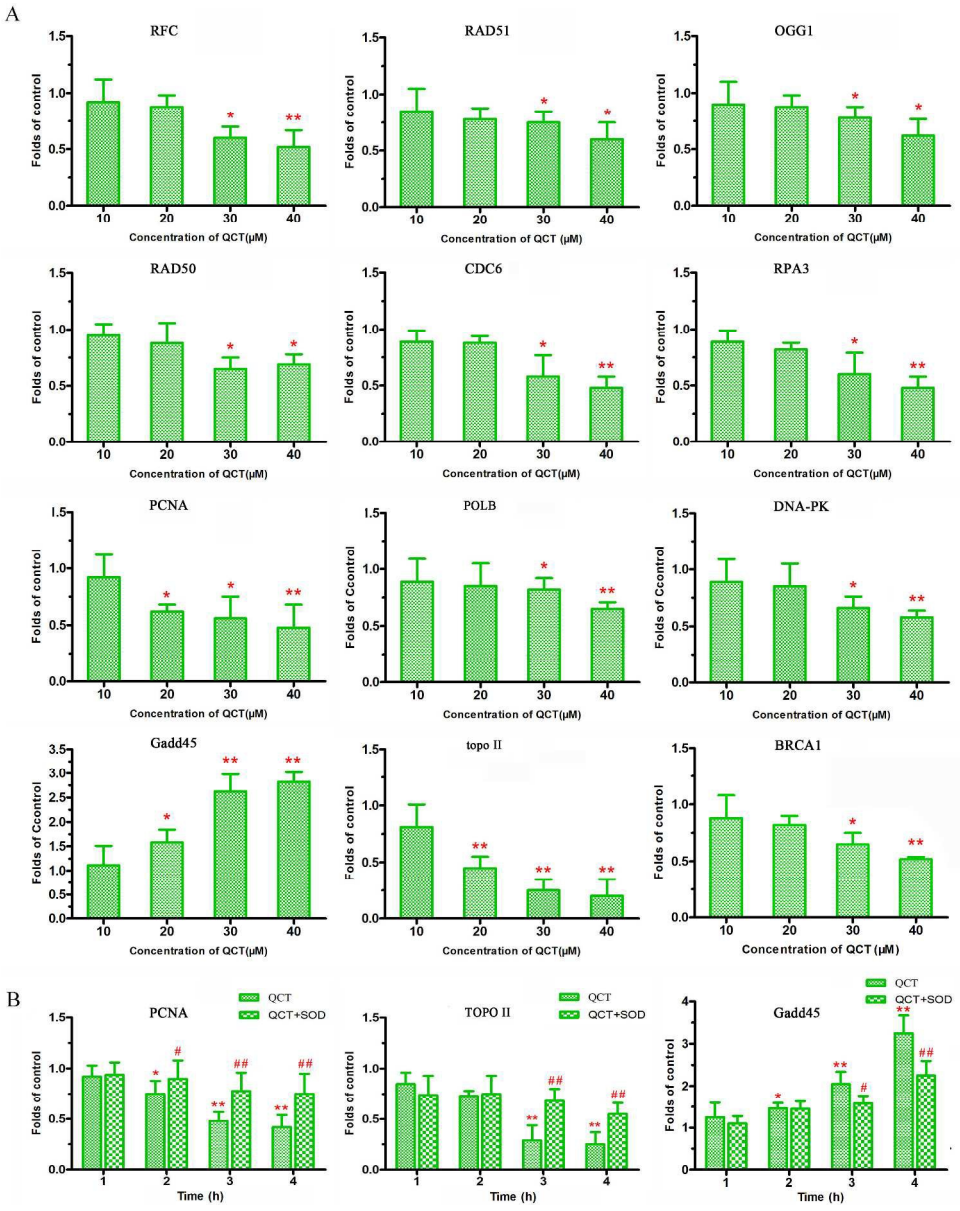

Fig. 7 Level of expression of DNA replication and repair genes in HepG2 cells treated with various concentrations of quinocetone (QCT). (A) Cells treated with QCT at 10, 20, 30 and 40 μM for 4 h. (B) Cells treated with QCT at 40 μM and 3.25 U/μL SOD for different exposure times. Data are means ± SD (n = 3). *P < 0.05 and **P < 0.01 vs. the blank control group; # P < 0.05 vs. the same dose in the QCT group.
288x360mm (300 x 300 DPI)

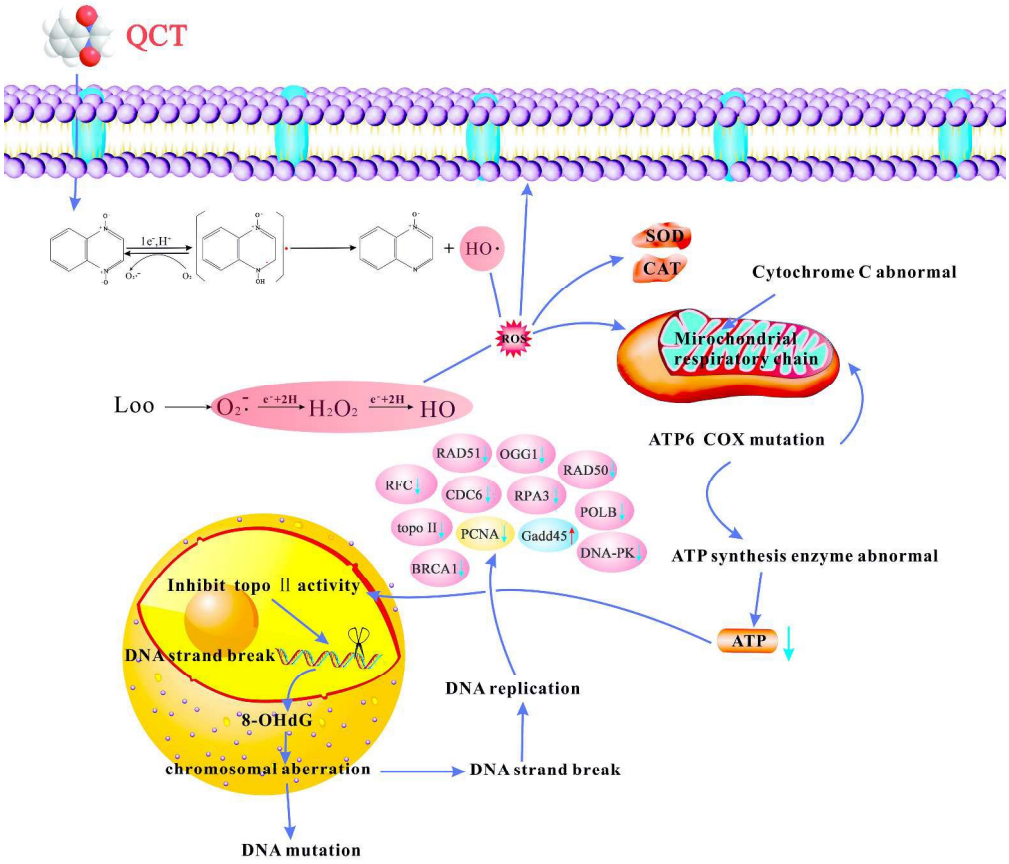

Fig. 8 The proposed mechanisms of the genotoxicity of quinocetone (QCT). The production of O2•- and OH• occurs via the reduction of the N-O group of QCT. After all defense systems are damaged, ROS can easily attack the mitochondrial DNA and cause gene mutations. Furthermore, QCT can also induce the generation of topoisomerase-DNA complexes and affect DNA replication.
438x381mm (300 x 300 DPI)

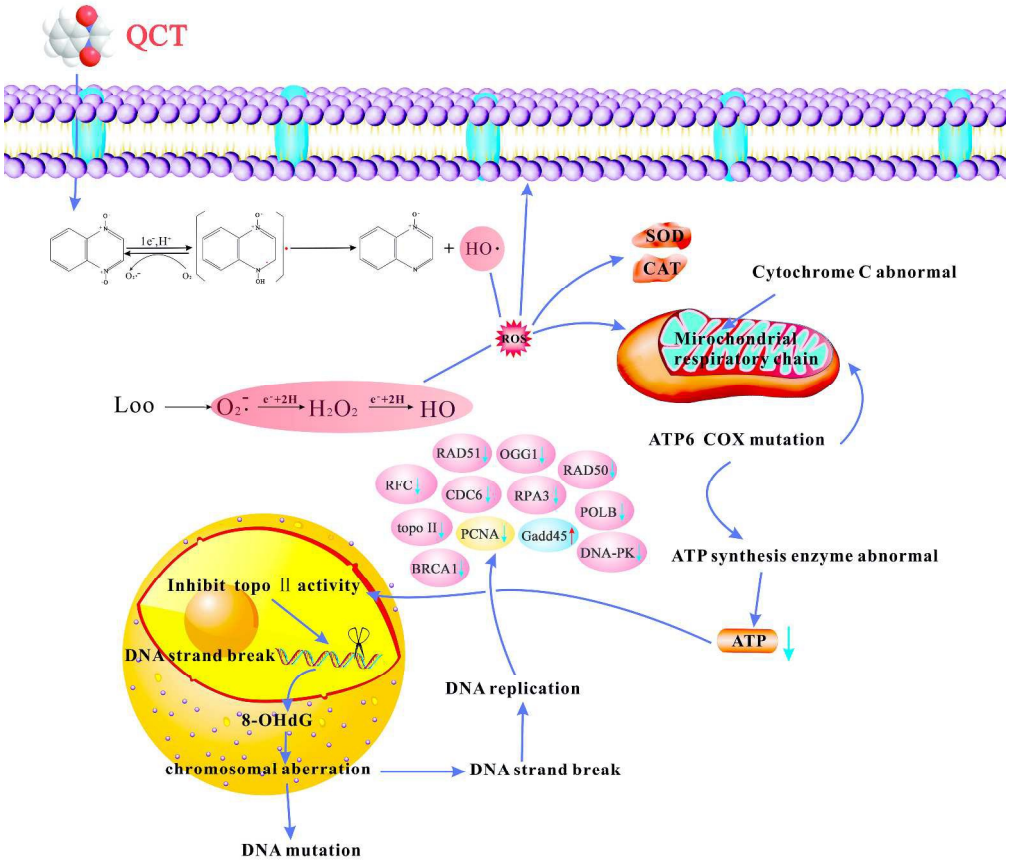

438x381mm (300 x 300 DPI)